Flexible and Printed Electronics

Conductance and spectroscopic mapping of EDOT polymer films upon electrochemical doping

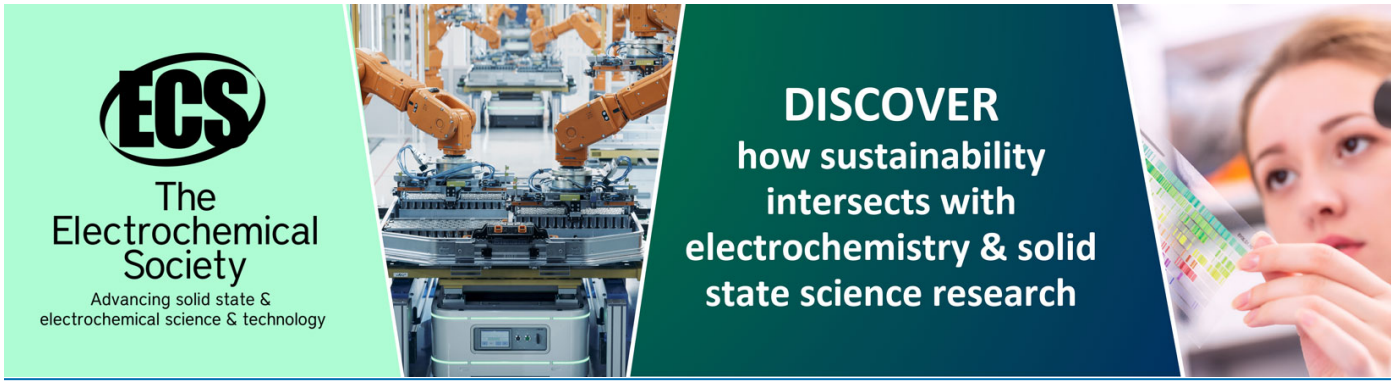

Flexible and Printed Electronics

PAPER

Conductance and spectroscopic mapping of EDOT polymer films upon electrochemical doping

Matthias Wieland[1,3], **Claudia Malacrida**[1,3], **Qiulin Yu**[1], **Claire Schlewitz**[1], **Luca Scapinello**[1,2], **Andrea Penoni**[2] **and Sabine Ludwigs**[1]

[1] IPOC—Functional Polymers, Institute of Polymer Chemistry, University of Stuttgart, Germany
[2] Dipartimento di Scienza e Alta Tecnologia, University of Insubria, Italy
[3] These authors contributed equally to the manuscript

E-mail: sabine.ludwigs@ipoc.uni-stuttgart.de

OPEN ACCESS

RECEIVED
13 October 2019

REVISED
18 December 2019

ACCEPTED FOR PUBLICATION
17 February 2020

PUBLISHED
23 March 2020

Keywords: OECT, PEDOT, cyclic voltammetry, spectroelectrochemistry, mixed-valence conductivity

Supplementary material for this article is available online

Abstract

This paper deals with the electrochemical doping of different poly(ethylenedioxythiophene) (PEDOT)-based active layers performed in an organic electrochemical transistor configuration through the mapping of *in situ* conductance trends during electrochemical doping and dedoping. The experiments are complemented by UV/Vis/NIR *in situ* spectroelectrochemistry in the wavelength range from 400 to 1600 nm, which allow monitoring of the development of the neutral and charged redox species. Both electropolymerized EDOT-based layers and solution-processed chemically synthesized PEDOT films are characterized. In addition to pure electropolymerized PEDOT (e-PEDOT), tris(4-(2,3-dihydrothieno[3,4-b][1,4]dioxin-5-yl)phenyl) (TPA-$EDOT_3$) is electrodeposited to generate highly branched networks of P(TPA-$EDOT_3$). The solution-deposited PEDOT films contain poly(ethylenedioxythiophene):poly(styrenesulfonate) (PEDOT:PSS) with ratios of 1:2.5 and 1:6. Overall, we find that e-PEDOT and PEDOT:PSS(1:2.5) behave like classical conjugated polymers with a plateau-like conductance over a wide potential region. In contrast, PEDOT:PSS(1:6) and P(TPA-$EDOT_3$) show rather bell-shaped conductance profiles. The mixed-valence conductivity model is used to interpret the experimental results in terms of the number of accessible redox states. We suggest that the bell-shaped conductance in the case of PEDOT:PSS(1:6) is caused by a high amount of PSS insulator that limits the inter-chain interaction between PEDOT moieties and in the case of P(TPA-$EDOT_3$) by its distorted molecular architecture.

1. Introduction

Organic electrochemical transistor devices (OECTs) are gaining more and more interest due to their promising applications in biosensors and bioelectronics [1]. Materials that show a change in electronic conductivity upon oxidation/reduction are suitable for use as the active layer in OECTs, since the change in the electronic conductivity can be utilized for the current switching function in the devices [2]. Semiconducting polymers, generally classified into conjugated and redox polymers, are perfect candidates for the active layers because of their ability to reversibly switch between the neutral and the doped states. In these systems, conducting states can be obtained by oxidation/reduction of the polymer backbone in the case of conjugated polymers, or of the redox-active moieties in the case of redox polymers. Since electrochemical charging or doping requires counterbalancing with ions to maintain electroneutrality, the polymer layers used in OECTs also have to allow ion exchange with an electrolyte.

OECTs can be driven in the accumulation or the depletion mode. On the one hand, conjugated polymers such as poly(3-hexylthiophene) (P3HT) that are in the neutral state and thus non-conducting state have to be oxidized in order to enable a drain current to flow (accumulation mode) [3]. On the other hand, materials that are already oxidized and thus conducting in their pristine state, such as poly(3,4-ethylene-

dioxythiophene):poly(styrenesulfonate) (PEDOT:PSS), enable drain current and thus the transistor is in its on-state without any applied voltage [4]. In this second case, only upon reduction of the pristine charged states, the drain current and thus the transistor can be switched off (depletion mode). Further in-depth information about OECTs can be found in a recent review by Rivnay *et al* [1].

The first experiment for measuring electronic conductivity of electroactive thin films during electrochemical experiments, commonly called *in situ* conductance, was developed by Zotti *et al* [5]. This method was based on the use of a double-band microelectrode separated by an insulator with known spacing (in the μm range) and the concurrent use of two potentiostats. The double-band microelectrode acts as the working electrode in a three-electrode configuration and allows electrochemical measurements. Simultaneously, the conductance of an electroactive film deposited on the electrode surface and bridging the two bands is mapped as a function of the polarization potential of the electrochemical experiment. Wrighton *et al* subsequently improved Zotti's set-up for potential-dependent conductance evaluation by replacing the band arrangement with an interdigitated microarray configuration which allows more sensitive determinations of currents [6–8], as shown in scheme 1. Different polymer materials including polyaniline [9], polypyrrole [10] and polythiophene derivatives [11, 12] have since then been characterized with this electrochemical set-up. The technique is for example reviewed in references [13] and [14]. Our groups have used cyclic voltammetry (CV) coupled with *in situ* conductance measurements of pure redox polymer systems, such as triphenylamine (TPA)-bearing polymers in order to study mixed-valence conductivity [15, 16]. While the conductance profile of the conjugated polymers is typically plateau-like, the redox polymers show conductance maxima only at specific potentials, which strongly depend on the degree of doping and therefore accessible redox states.

Among the conjugated polymers, poly(ethylenedioxythiophene) (PEDOT) remains one of the most widely utilized materials. Both electrochemical and chemical synthesis routes have been shown in literature and discussed extensively [4, 17]. In the case of electropolymerization, PEDOT can be obtained from EDOT-monomer containing electrolytes directly onto electrode surfaces. The nature of the electropolymerization product can be tuned by the choice of electrolyte and electrodeposition techniques [13]. Depending on the oxidation level PEDOT can be in the neutral, radical cation and dication states, often referred to as non-doped, polaron and bipolaron states, respectively; see figure 1.

As solution-processable material poly(ethylenedioxythiophene):poly(styrenesulfonate) (PEDOT:PSS) is of highest relevance in the field of polymer electronics. PEDOT:PSS is synthesized via oxidative polymerization in aqueous PSS solution and is essentially a complex of PEDOT in its doped state and the ionically conducting polyelectrolyte PSS as polymeric counter-ions [4]. Depending on the ratio of PEDOT to PSS, different applications can be realized; whereas the 1:2.5 ratio is often used as electrode replacements [18], the 1:6 ratio can be utilized as an interlayer in organic photovoltaics [19] or organic light-emitting diodes [20]. In dispersion, PEDOT:PSS forms colloidal gel particles, which result after coating on a substrate in PEDOT-rich and PSS-rich phases [21, 22]. We refer to Modarresi *et al* who give a good summary of current morphological models [23].

In the current study, we compare the electrochemical doping behavior of films of electropolymerized EDOT materials and spin-coated PEDOT:PSS with PEDOT to PSS ratios of 1:2.5 and 1:6. In addition to pure electropolymerized PEDOT (so-called e-PEDOT), the last part of the manuscript will deal with the electropolymerization product of tris (4-(2,3-dihydrothieno[3,4-b][1,4]dioxin-5-yl)phenyl) P(TPA-EDOT$_3$) which is an example of a three-dimensional redox polymer where bi-EDOT units are connected by triphenylamine (TPA) core units; see supporting information available online at stacks.iop.org/FPE/5/014016/mmedia and figure 3(a). CV is coupled with *in situ* conductance and *in situ* UV/Vis/NIR absorption spectroscopy (400–1600 nm) measurements, which allows us to follow the trends in conductance as a function of the charging level and to follow the evolution of the neutral, polaron (radical cation) and bipolaron (dication) species at the same time. These experiments also allow us to screen different materials for their suitability in real OECT device operations, because they provide information about the potential range in which EDOT polymers are in their most conducting state.

2. Experimental procedures

2.1. Film preparation on working electrode

Pt interdigitated microarray electrodes (from Fraunhofer Institute of Physical Measurement Techniques IPM) with channel lengths of 5 μm and channel widths of 192 cm were cleaned twice for five minutes in acetone with ultrasonification. Two PEDOT:PSS batches were used for film preparation; firstly, a Clevios PVP AI 4083 batch (PEDOT to PSS weight ratio 1:6, in the following referred to as PEDOT:PSS (1:6)) and, secondly, a Clevios PH 1000 batch with a 1:2.5 weight ratio referred to as PEDOT:PSS(1:2.5), both from Heraeus. Films from these materials were prepared by spin-coating from 15 μl aqueous suspensions of PEDOT:PSS(1:6) with 3000 rpm and 1500 rpm for PEDOT:PSS(1:2.5). The film thicknesses of these spin-coated films are typically in the range of 70–80 nm as measured by profilometry. Before further use, the films were dried for at least 10 min under

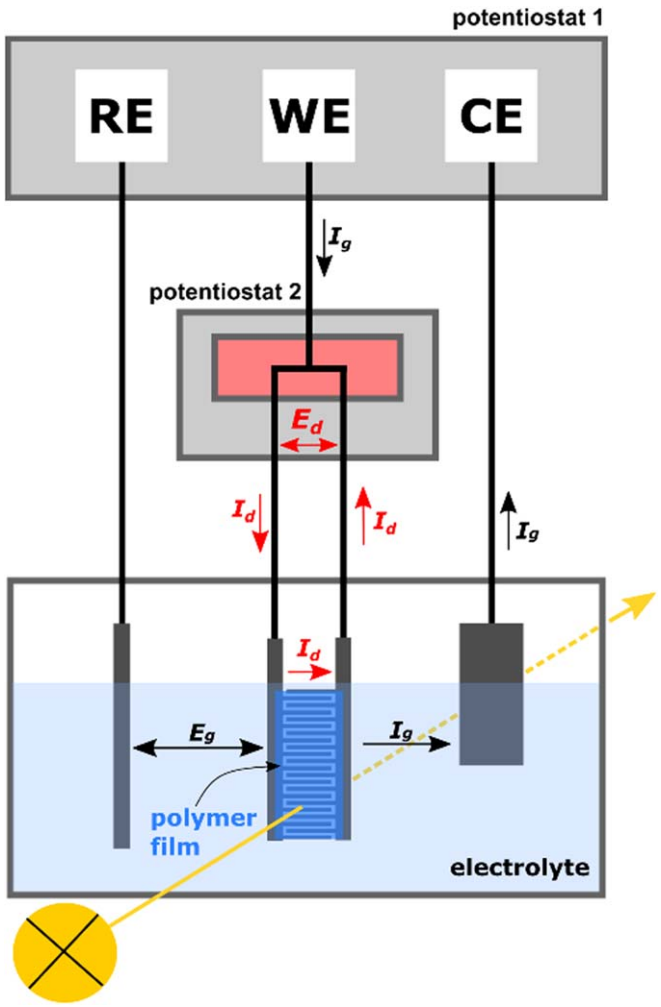

Scheme 1. Scheme of electrochemical set-up for coupling CV (WE, RE and CE refer to working, reference and counter electrode) with *in situ* conductance and/or *in situ* UV/Vis/NIR absorption spectroscopy, in which E_g is the gate potential (electrochemical doping potential), I_g the gate current, E_d the drain potential and I_d the drain current. E_d is fixed to 10 mV, and Ohm's law is used to calculate the conductance.

vacuum. e-PEDOT was prepared by CV (see electrochemical methods) by applying eight cycles in a potential range between −1.3 V and +1 V versus Ag/AgCl in 10 mM EDOT. The synthesis of TPA-EDOT$_3$ was conducted according to procedures in literature and involves a stannylation of EDOT [24] and subsequently a Pd catalyzed Stille cross-coupling reaction with TPA [25]. Details about the synthesis can be found in the supporting information. Electropolymerized P(TPA-EDOT$_3$) films were prepared with CV by applying five cycles in a potential range between −0.5 V and +1.2 V versus Ag/AgCl in a 5 mM solution of TPA-EDOT$_3$ in 1:1 dichloromethane/acetonitrile (typical film thicknesses of the electropolymerized films are around 500 nm).

2.2. Electrochemical methods

For electrochemical measurements, three-electrode set-ups with a Pt counter-electrode (CE) and an AgCl-coated Ag wire as the reference electrode (RE) with a potentiostat from Metrohm were used. All measurements were referenced to the external intersolvential standard Fc/Fc^+. As an electrolyte a 0.1 M solution of tetrabutylammonium hexafluorophosphate (NBu_4PF_6) in acetonitrile (MeCN) was used. All measurements were conducted in an argon atmosphere. CV measurements with *in situ* conductance measurements and *in situ* UV/Vis/NIR absorption spectroscopy measurements were conducted with the polymer film-coated interdigitated electrodes as working electrodes (WE), as shown in scheme 1. For measuring the *in situ* conductance we use a commercial set-up from Metrohm in which a potential of 10 mV is applied by potentiostat 2 (μStat400 from DropSense) between both sides of an interdigitated electrode (E_d), and the current (I_d) is measured as function of the potential in the CV measurement potentiostat 1 (Autolab PGSTAT204 from Metrohm). With the help of two resistors (interface from Heka) both signals are galvanostatically separated in order to allow us to conduct both the CV measurements and to measure the *in situ* conductance simultaneously. Note that throughout the study we only discuss conductance trends and not absolute values since background currents cannot be neglected in this measurement

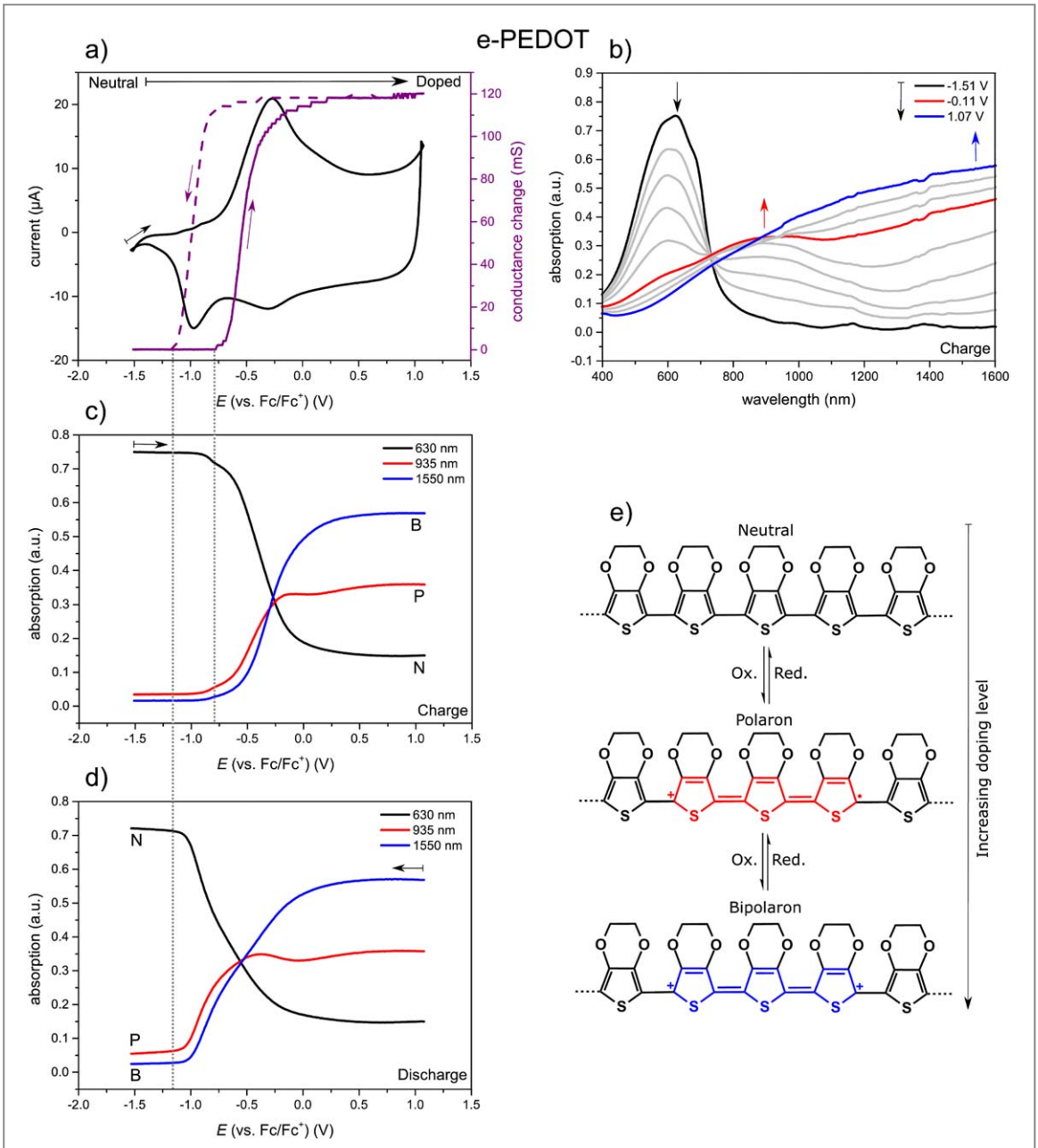

Figure 1. *In situ* studies of e-PEDOT. (a) CV (black line) and *in situ* conductance (charge sweep violet solid line, discharge sweep violet dashed line). (b) UV/Vis/NIR absorption spectra during charge sweep at various potentials. Peak trend (evolution of peak absorption) of neutral band at 630 nm (black), polaron band at 935 nm (red) and bipolaron band at 1550 nm (blue) extracted from the absorption spectra during charge (c) and discharge (d) sweeps. (e) Chemical structures of neutral, polaron and bipolaron states on PEDOT chains. All measurements were conducted in 0.1 M NBu_4PF_6/MeCN at a scan rate of 10 mV s^{-1}.

configuration. *In situ* conductance values are given as conductance change with respect to the conductance of the materials in the neutral state.

For the *in situ* UV/Vis/NIR spectroelectrochemistry measurements of the polymer films either the interdigitated electrodes were directly connected as the working electrode or ITO electrodes were used. The measurements were conducted in a quartz cell and the *in situ* absorption was measured by connecting the light source and the detector on opposite sides of the cell. For all films, the *in situ* conductance measurements were conducted prior to the *in situ* UV/Vis/NIR absorption spectroscopy measurements. The data shown in this contribution are all taken from the second cycles in order to eliminate memory effects that might occur in the first cycle [26].

3. Results and discussion

3.1. *In situ* studies of e-PEDOT

As the first step we electrodeposited EDOT according to standard electropolymerization procedures by CV to obtain overall neutral e-PEDOT films [27, 28]. As the supporting electrolyte NBu_4PF_6 in acetonitrile was used, and eight cycles were applied. The electropolymerization of EDOT proceeds in a kind of step-growth polymerization manner and e-PEDOT can be

regarded as a mixture of different chain lengths of EDOT sequences. One of the best models to describe the electropolymerization is the so-called oligomer approach [13]. It is important to mention that during cycling the charges on the polymer backbone are counterbalanced by ions from the electrolyte, which is also accompanied by solvent uptake [13]. Acetonitrile is a very suitable solvent for electrochemical experiments because of its large electrochemical window which allows oxidation and reduction of PEDOT over a wide potential range. Potentiodynamic cycles are terminated at potentials for which the polymer is in its neutral state. All of the following studies are performed in monomer-free electrolyte.

In figure 1(a), the CV and the corresponding *in situ* conductance measurements of neutral e-PEDOT films are shown. The voltammogram itself shows the typical broad signal of electropolymerized conjugated polymer films with an onset of oxidation of −1.15 V. The e-PEDOT is oxidized from the neutral state into charged states upon increase of the potential and can be reversibly reduced to its neutral state. During the experiment the charges on the backbone are neutralized by the electrolyte [13]. In the simplest case PF_6^- is counterbalancing the positive charges, even though the real situation is presumably more complicated and could be further elucidated with advanced techniques like AC gravimetry [29].

The simultaneously recorded conductance change suggests that the oxidation of e-PEDOT leads to a change from a low to a non-conducting to a conducting state, with a typical sigmoidal variation of the conductance as a function of the doping level [13, 30]. In concomitance to the oxidation onset in the CV charge carriers are generated in the polymer backbone and an increase in the conductance is observed which results in a plateau at higher oxidation potentials. The process is reversible for the discharge step, as the *in situ* conductance decreases again in the neutral state. The *in situ* conductance of the electropolymerized PEDOT studied here is at its maximum over a broad potential range from 0.2 to 1.0 V versus Fc/Fc^+. This high conductance over a broad potential window is typical for conjugated polymers [13].

As already mentioned, to better understand and interpret the *in situ* conductance behavior, the analysis of spectroscopical variation of the film upon doping is a very useful tool for the assignment of the respective charge carriers to the doping level of the polymer film. In figure 1(b), the *in situ* UV/Vis/NIR spectra registered during the charge step of e-PEDOT are given. For e-PEDOT as well as for all other PEDOT materials in this contribution, the UV/Vis/NIR spectra of the respective charge or discharge sweeps are given in addition in the supporting information. At a potential of −1.51 V (black curve in figure 1) e-PEDOT is characterized by one broad absorption band with a maximum at 630 nm which can be assigned to neutral PEDOT. As the electrochemical polarization potential is increased and the polymer starts to become oxidized, two new absorption bands at 935 nm and 1550 nm appear, with a concurrent decrease in the intensity of the neutral band at 630 nm. The mid-energy band (935 nm) and the low energy band (1550 nm) are assigned to polaron and bipolaron species, respectively, in agreement with the literature [4, 31–35]; see also figure 1(e). In figures 1(c) and (d), the peak trends (evolution of peak absorption) of the neutral band and the polaron and bipolaron bands at 935 nm and 1550 nm for the charge and discharge processes are shown. Looking at the peak trend for the polaron band during the charge scan, a slight maximum is observed at potentials of ∼−0.14 V which could suggest a maximum of the polaron species, as shown in figure 1(c). At higher potentials the superposition of the 935 and 1550 nm bands makes it difficult to separate and to determine their relative contributions. In this context, Zozoulenko *et al* showed with the help of density functional theory calculations that electronic polaron and bipolaron transition contributions are existent both at low and high oxidation levels, in which the spin count and thus the polaron transition exhibits a maximum at intermediate oxidation potentials [36].

The *in situ* conductance shows a hysteresis between the charge and the discharge scans as a function of potential, i.e. for the charge scan the *in situ* conductance starts to increase at potentials above −0.77 V and for the discharge scan the *in situ* conductance reaches its minimum at potentials below −1.15 V. This trend is also visible in the absorption spectra: the absorption of the neutral band starts decreasing at potential values more positive than −0.89 V in the charge sweep, whereas during the discharge sweep, the neutral absorption reaches its maximum for potential values more negative than −1.09 V.

3.2. *In-situ* studies of PEDOT:PSS

The following section is dedicated to the characterization of the solution-deposited chemically polymerized PEDOT:PSS. Since synthesis of PEDOT:PSS is based on an oxidative polymerization, similar PEDOT materials are expected as for the e-PEDOT case [17]. The main difference is that in the case of PEDOT:PSS a polymeric anion is involved which is immobilized in the PEDOT:PSS mixture while in the above studied e-PEDOT the ions from the NBu_4PF_6 salt are incorporated in the film in order to establish charge neutrality.

The results from the *in situ* UV/Vis/NIR and conductance studies of PEDOT:PSS(1:2.5) and PEDOT:PSS(1:6) are summarized in figure 2. Since PEDOT:PSS is in its fully oxidized state at ambient conditions, all measurements were performed starting with the discharge sweep of the CV experiment, which means that PEDOT:PSS is reduced from the oxidized to the neutral state with decreasing the electrochemical potential.

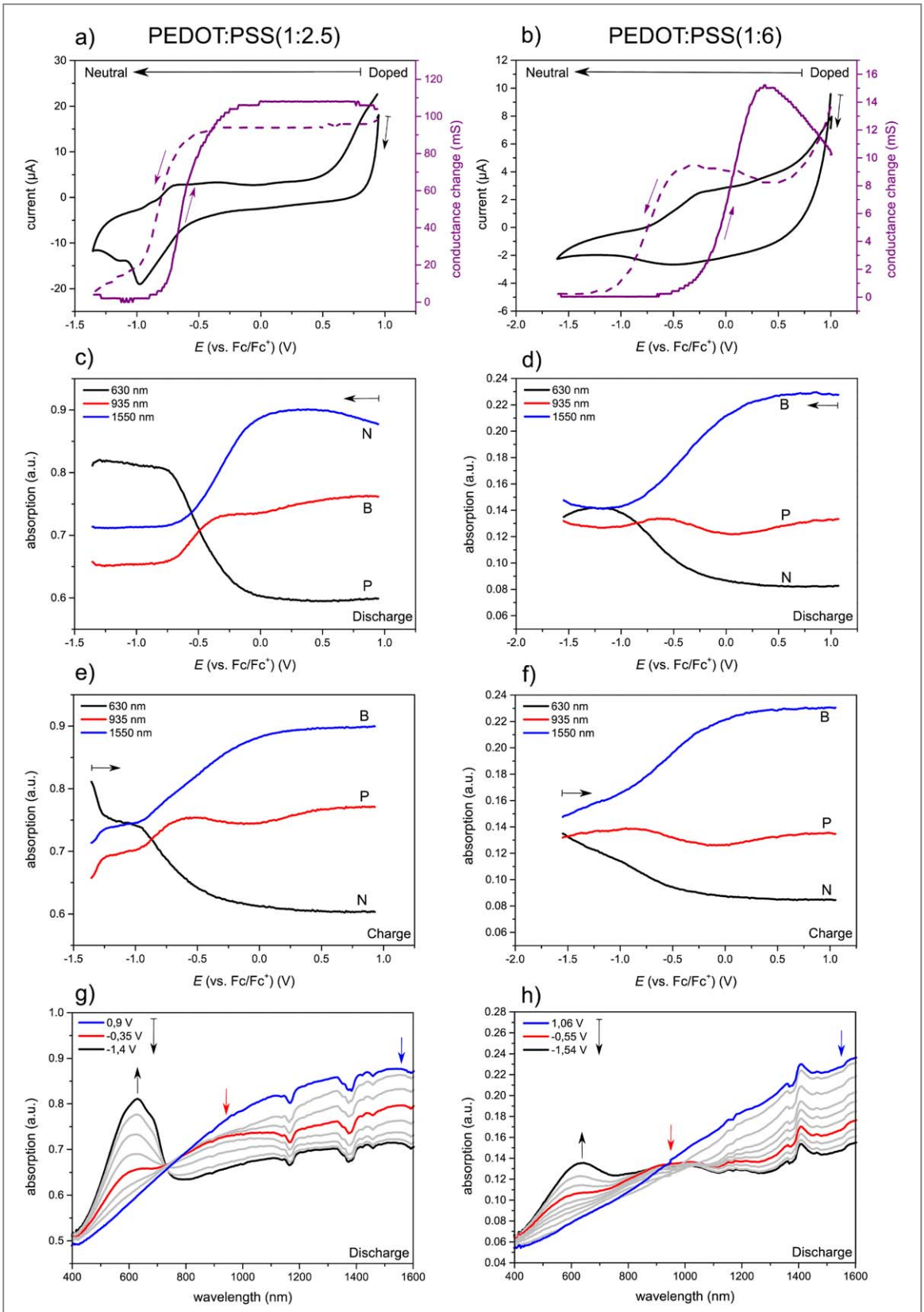

Figure 2. *In situ* studies of PEDOT:PSS(1:2.5) in (a), (c), (e) and (g) and PEDOT:PSS(1:6) in (b), (d), (f) and (h). CV and *in situ* conductance (discharge sweep dashed violet line, charge sweep violet solid line) of (a) PEDOT:PSS(1:2.5) and (b) PEDOT:PSS(1:6). Peak trend (evolution of peak absorption) of neutral (black), 935 nm polaron band (red) and 1550 nm bipolaron band (blue) extracted from the absorption spectra during discharging and charging for PEDOT:PSS(1:2.5) in (c) and (e) and for PEDOT:PSS(1:6) in (d) and (f). (g) and (h) are the corresponding *in situ* spectra during discharge for PEDOT:PSS(1:2.5) and PEDOT:PSS(1:6), respectively. All measurements were conducted in 0.1 M NBu_4PF_6/MeCN at a scan rate of 10 mV s^{-1}.

3.2.1. PEDOT:PSS(1:2.5)

The CV of PEDOT:PSS(1:2.5) in figure 2(a) shows multiple waves, which is typical for conjugated polymers. In the discharge sweep two main reduction peaks around −0.98 V and −1.18 V can be distinguished. The corresponding oxidation peaks are encountered in the charge sweep at around −0.92 V and −0.72 V. A third oxidation peak is present at around −0.45 V; however, the reduction counterpart cannot be clearly identified.

The *in situ* conductance of PEDOT:PSS(1:2.5) shows a trend which is overall very similar to the one observed for e-PEDOT: a change from a conductive state at positive potentials to low conductance upon discharge. The polymer shows its maximum conductance in a broad potential region with a plateau-like behavior encountered for potential values superior to −0.30 V in the case of the charge sweep, and superior to −0.60 V in the case of the discharge sweep. The variation in the conducting properties of the polymer are compared with the spectroscopic variations registered on the same sample during *in situ* UV/Vis/NIR spectroelectrochemistry; see figures 2(c), (e), (g). Similar UV/Vis/NIR absorption patterns are also encountered for PEDOT:PSS(1:2.5) and e-PEDOT, suggesting that the two materials have similar electronic nature of the different PEDOT moieties in their neutral (630 nm, black curve), polaron (935 nm, red curve) and bipolaron (1550 nm, blue curve) states. The presence of PSS in the films of PEDOT:PSS(1:2.5) does not seem to result in changes of the overall absorption characteristics of PEDOT.

The peak trend of neutral, polaron and bipolaron bands of PEDOT:PSS(1:2.5) for the discharge (figure 2(c)) and charge sweep (figure 2(e)) show a reversible redox switching of PEDOT:PSS(1:2.5) with a hysteresis of 0.6 V. The peak evolution is also comparable to that of e-PEDOT. A full conversion to neutral PEDOT is reached for the discharge process at potentials more negative than −0.75 V, when the absorption band at 630 nm reaches its maximum concurrently with the complete bleaching of the polaron and bipolaron bands. A peculiarity is observed during the charge sweep (figure 2(e)): in the potential range between −1.4 V and −1.27 V the absorption of the neutral peak decreases significantly, while the absorption of polaron and bipolaron bands increases. The absorption of the bands then remains constant until the potential value of −0.95 V is reached, after which the absorption of the neutral band further decreases and the absorption of both polaron and bipolaron bands rise. The variation of the absorption properties encountered for potentials more positive than −0.95 V is in good agreement with the onset of the conductance (−0.90 V). This stepwise change in the absorption can also be observed on ITO electrodes (supporting figure S3) and has not been previously discussed in the literature.

3.2.2. PEDOT:PSS(1:6)

The cyclic voltammogram of PEDOT:PSS(1:6) which contains PSS as a majority component shows rather indistinct waves and a tilt in the baseline, which might be explained by a higher internal resistance with respect to the higher PEDOT content e-PEDOT and PEDOT:PSS(1:2.5) materials [37]. In contrast to the other analyzed systems where a conductance plateau was found for high doping levels, in the case of PEDOT:PSS(1:6) a broad bell-shaped conductance trend is encountered (figure 2(b)). The conductance maxima are found at −0.30 V for the discharge sweeps and at 0.39 V for the charge sweep. The significant hysteresis observed between the conductance maxima (difference of ~0.7 V) might also be explained by the higher internal resistance due to the large amount of PSS.

The *in situ* spectra of PEDOT:PSS(1:6) are presented in figure 2(h) showing analogies with the other PEDOT samples. The maxima of absorption for the neutral (630 nm), polaron (935 nm) and bipolaron (1550 nm) states do not differ from the maxima of the other PEDOT materials previously discussed. During the discharge sweep, in spite of going to rather negative potential values (−1.54 V) the polaron band (935 nm) of PEDOT:PSS(1:6) is still observed together with the neutral band (630 nm). The peak maximum variation with the potential for the PEDOT:PSS film is presented in figure 2(d) (discharge cycle) and f (charge cycle). The same effects were also observed during the *in situ* UV/Vis/NIR absorption studies on ITO substrates (figure S4). Further, only small changes during the discharge and charge sweep are found in the peak trend of the polaron band (figures 2(d) and (f)), hinting at an incomplete conversion of bipolaron and polaron states to neutral state.

3.2.3. Comparison of PEDOT:PSS ratios

A huge amount of research on PEDOT:PSS in the literature is dedicated to electronic conductivity optimization for their use as electrode replacements in flexible electronic devices [38, 39]. Zotti *et al* compared electropolymerized PEDOT and PEDOT:PSS with *ex situ* conductivity measurements of the pristine PEDOT films and CV with *in situ* UV/Vis/NIR absorption spectroscopy [17]. They found that the conductivity of electropolymerized PEDOT is significantly higher than that of pristine chemically synthesized PEDOT:PSS. The experimental results were explained with the amount of insulating counter-ions in the composite PEDOT:PSS materials: whereas only the minimum amount of required counter-ions is included in the film formation during an electropolymerization, an excess amount of polymeric PSS anions is present in PEDOT:PSS films. While the conductivity of PEDOT:PSS(1:6) is overall quite low, which is indeed due to the high PSS content [40], PEDOT:PSS batches with 1:2.5 or 1:2.2 ratios can be manipulated to be highly conducting up to values as high as

4380 S cm^{-1} [41]. Approaches include for example processing with additives or post-processing technologies [21, 42, 43].

In the present work we found that different PSS contents strongly influence the ability of the system to be discharged to the neutral state. This is evidenced for example by the immediate stepwise conversion of PEDOT:PSS from the neutral to the oxidized state in the charge sweep of PEDOT:PSS(1:2.5) and by the inability to fully discharge PEDOT:PSS(1:6) (figure 2(c)). Analogous results were encountered during experiments performed on ITO electrodes; see figures S3 and S4. These experimental observations could be explained by the presence of immobile negatively charged PSS moieties forced into close proximity of the polymer backbone stabilizing its oxidized state [21, 43, 44]. Indeed, in the case of e-PEDOT where the ions counterbalancing the positive charges are provided entirely by the electrolyte ions (NBu_4PF_6), a complete discharge of the polymer film can be performed. The ability of the different PEDOT materials to be discharged is evidenced by the absorption spectra registered at negative potentials. In this situation, e-PEDOT shows only the neutral band whereas in the extreme case of PEDOT:PSS(1:6) the polaron band is still encountered together with the neutral one.

Further, we found that in the extreme case of PEDOT:PSS(1:6) the low PEDOT content also seems to influence the potential-dependent conductance behavior of the material, which shows a bell-shaped conductance profile. The experimental results on e-PEDOT and PEDOT:PSS(1:2.5) on the other hand seem to be in accordance with the majority of cases encountered during *in situ* conductance experiments of conjugated polymers, where a plateau-like behavior of high conductance is found for high doping levels. The broad *in situ* conductance maximum could be described with the model proposed by Heinze *et al* considering the conjugated polymer to be composed by multiple and overlapping interacting mixed-valence states, each of which is passed as the polymer is charged [13]. The polymer system can then be considered to be always in a mixed-valence state [13]. This is reasonable as mixtures of different chain lengths (molecular weights) and effective conjugation lengths are present in the conjugated polymer films. Both multiple effective conjugation and intermolecular interactions in these systems seem to contribute to give high conductance over large potential windows. In the literature, a decrease of the *in situ* conductance at very high potentials is further observed [45, 46]. The absence of mixed-valence states for hopping at high doping levels might explain this phenomenon. Therefore, it is reasonable to apply the mixed-valence conductivity model for the case of conjugated polymers from an electrochemical perspective [13]. For complementarity we mention here the older bipolaron model [26, 47–49].

In the case of PEDOT:PSS(1:6), a bell-shape behavior during the *in situ* conductance experiments is found. We explain the observed behavior in the context of the mixed-valence conductivity model, as the amount of available or interacting redox states seems to be significantly smaller in the high PSS content polymer than for e-PEDOT and PEDOT:PSS(1:2.2). A possible explanation might include the hindered electronic interactions between PEDOT phases in PEDOT:PSS due to large amounts of electronically insulating PSS in the polymer blend. This hindrance is dependent on the ratio of PEDOT to PSS as seen by the decrease in electronic conductivity with increasing PSS content [40]. We refer to the morphology models in literature on phase-separated structures of PEDOT and PSS domains [21, 22]. Furthermore, as discussed by Fan *et al* and Ju *et al* the presence of PSS might imply the distortion of PEDOT molecular chains due to the different lengths of the polymer chains of PEDOT and PSS [43, 44]. Similar explanations were suggested by Rivnay *et al*: the addition of ethylene glycol to aqueous PEDOT:PSS suspensions increased phase separation between PEDOT-rich and PSS-rich moieties with optimized packing of the PEDOT domains [21]. The proposed distortion by PSS might therefore cause a decrease in the conjugation of PEDOT chains, which might also depend on the PEDOT to PSS ratio.

3.3. *In situ* studies of P(TPA-EDOT$_3$)

The peculiarities of PEDOT:PSS(1:6) as a system with partially localized redox centers with limited intermolecular interaction in an electronically insulating PSS matrix become further evident when comparing this system with P(TPA-EDOT$_3$). This polymer can be essentially regarded as a conjugated polymer with a limited conjugation length, since the propeller-shaped TPA separates bi-EDOT units (figure 3(a)).

The CV of P(TPA-EDOT$_3$) shows one broad oxidation and reduction wave (figure 3), which is in accordance with data from Chahma *et al* [25]. The authors measured *in situ* UV/Vis/NIR absorption and explained the broad redox waves by coinciding redox potentials of the bi-EDOT and the TPA unit. By comparing the oxidation potentials of different di- and triphenylamine aromatic heterocyclic compounds, they deduced that the oxidation potentials for the bi-EDOT and the triphenylamine moieties are very similar, which results in broad oxidation waves [50]. The UV/Vis/NIR spectra in the charge sweep (figure 3) show in the neutral state (black line) two absorption bands at 440 nm and 680 nm. The former can be assigned to π–π^* transitions and the latter to intramolecular sulfur–oxygen interactions. Comparing the neutral band of P(TPA-EDOT$_3$) with the neutral absorption of the PEDOT materials, figures 1(d) and 2(g) and (h), P(TPA-EDOT$_3$) reveals a band at 440 nm, while PEDOT absorbs around 600 nm. A

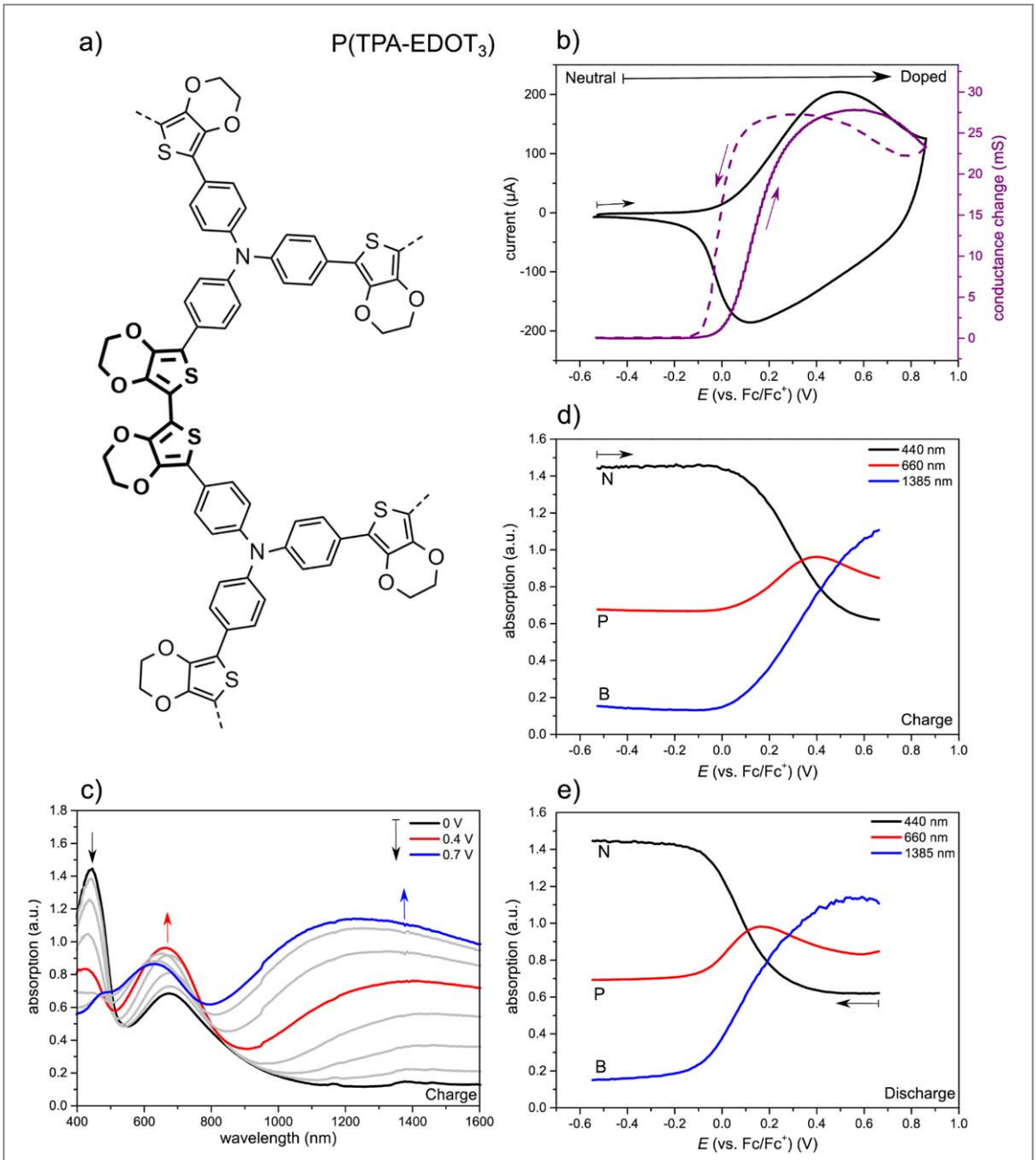

Figure 3. *In situ* studies of P(TPA-EDOT$_3$). (a) Chemical structure P(TPA-EDOT$_3$). (b) CV and *in situ* conductance (charge sweep, violet solid line; discharge sweep, violet dashed line). (c) UV/Vis/NIR absorption spectra of charge sweep at various potentials. Scan rate: 20 mV s^{-1}. (d) and (e) Peak trend (evolution of peak absorption) of neutral 440 nm band (black), 660 nm band (red) and 1385 nm band (blue) at charge (c) and discharge (d) sweep. (d) Evolution of conductance as function of the potential in a CV experiment of TPB-bearing redox polymers. All measurements were conducted in 0.1 M NBu_4PF_6/MeCN at a scan rate of 20 mV s^{-1}.

reasonable explanation is the overall shorter conjugation length in P(TPA-EDOT$_3$).

Upon oxidation (red and blue line), the intensity of the neutral band decreases and two bands at 660 nm and 1385 nm evolve; see figure 3(c). The peak trend of the charge sweep (figure 3(c)) shows that the neutral band starts to decrease simultaneously as the polaron and bipolaron bands start to increase. After a maximum of the polaron band at 0.57 V, the intensity decreases since the polaronic species are further converted into bipolaronic species. In the peak trend at the discharge sweep, the maximum of the polaron band is at 0.31 V, which means that the transition from the oxidized into the neutral state is shifted in the direction of the scan rate as seen in the hysteresis of the CV in figure 3(b).

In contrast to the plateau *in situ* conductance of e-PEDOT and PEDOT:PSS(1:2.5) and similarly to PEDOT:PSS(1:6), P(TPA-EDOT$_3$) shows a bell shape instead of a plateau in the *in situ* conductance trends. When analyzing the potential-dependent conductance behavior of the electropolymerized P(TPA-EDOT$_3$) system in relation to the peak trend of spectroelectrochemical measurements in figures 3(d) and (e),

an agreement with the model predicting multiple overlapping redox states, each of which following a mixed-valence conductivity model can be found. The maximum of conductance, broader than for canonical redox systems [51, 52], is indeed observed for the coexistence of different charged states, as shown in figures 3(d) and (e). As previously discussed in the text, an ubiquitous model for the description of potential-dependent conductance behavior of conjugated polymers has not yet been found [2, 13, 14]. A hypothesis for the conductance decrease observed here might be derived by the peculiar structure of the TPA-$EDOT_3$ monomer and its electropolymerization product. The TPA-$EDOT_3$ molecule is in fact endowed by an intrinsic 3D structure, imparted by the triphenylamine core. This tri-dimensional character is also transferred to the electropolymerization product.

It is well established that charge transport in conjugated polymers takes place both intra- and intermolecularly. In this context, the molecular structure, and in particular planarity, play a significant role. Both intra- and intermolecular transport pathways are in fact dominated by the torsional angle of the π-conjugated backbone, on which the effective conjugation and the extent of π-stacking depend. Due to the interrelation between these two factors, a clear separation between intra- and intermolecular contributions to conductivity is usually difficult to obtain [53]. We suggest that the bell-shaped conductance observed for electropolymerized P(TPA-$EDOT_3$) might be explained by the limited amount of total overlapping redox states in between which hopping takes place. The distorted nature of the repeating units could limit the effective conjugation of the system and the interchain interaction when compared to the linear PEDOT counterpart. A similar experimental observation was found by Benincori *et al* when studying *in situ* conductance of the electropolymerization product of an inherently chiral bis-EDOT derivative (2′-bis{bi [2,2′-(3,4- ethylenedioxy)thiophen-5-yl]}-3,3′-bithianaphthene) [54]. In their work two independent maxima of conductance are observed and described in terms of mixed-valence conductivity behavior between tetrameric EDOT units in their polaron and bipolaron state, respectively. The encountered similarity might be explained by the limited conjugation in the molecules determined by the atropoisomeric core, imparting a helicoidal geometry to the system and limiting the conjugation in the electropolymerization products only to tetrameric EDOT units. Different examples of oligomeric systems presenting mixed-valence conductivity behavior can be found in the literature including different oligo- and electropolymerized terthiophene-functionalized dendrimers studied by the Heinze group [15, 55]. As a final consideration, we refer to the conductance behavior of pure redox polymer films based on tetraphenylbenzidine (TPB) redox units crosslinking neutral vinyl and styrene polymer backbones [15, 16]. The *in situ* conductance during oxidation in a cyclic voltammetry experiment shows two overlapping conductance maxima. The results were explained by the authors in terms of mixed-valence conductivity, in particular the two partially overlapping maxima are attributed to the presence of half-neutral/half-radical cation (first maximum), and half-radical cation/dication species (second maximum), as the maxima coincide with the half-way potential of the corresponding redox species.

4. Conclusions

Within the article we have discussed *in situ* conductance and *in situ* UV/Vis/NIR spectroelectrochemistry of different EDOT-containing polymer films in OECT configurations. Both e-PEDOT and PEDOT:PSS(1:2.5) show broad sigmoidal conductance profiles, as many redox states are accessible in the polymer films contributing to the charge transport. This is due to the presence of mixtures of different chain lengths (molecular weights) and effective conjugation lengths. The spectroscopy data suggest the presence of both polaron and bipolaron species across the high conductance plateau in these systems which might be explained by mixed-valence conductivity [13, 48]. The intermolecular interactions and effective conjugation allow the systems to remain conducting over large potential windows.

In the case of PEDOT:PSS(1:6) the high amount of electronic insulator PSS within the mixtures seems to reduce intermolecular interactions between the PEDOT moieties. This might explain the bell-shaped conductance which is more typical for isolated redox sites in redox polymers. For P(TPA-$EDOT_3$) the conjugation lengths are limited due to the distorted character of the TPA core units.

In conclusion, we suggest that the mixed-valence conductivity model can be used to describe the potential-dependent conductance of all the systems analyzed here. These systems only differ in the availability of redox states due to factors such as the effective conjugation lengths, polydispersity, and the extent of intermolecular interactions. In general, the broadness of the conductance window is likely to be determined by the amount and superposition of subsequent redox states available.

These studies clearly show the relevance of analyzing the potential-dependent conductance behavior of conducting polymers in order to drive OECTs efficiently. *In situ* conductance allows precise identification of the potential range in which the switch between non-conducting (neutral) and conducting (oxidized) states occurs in the polymer.

Acknowledgments

We thank Professor J Heinze for having introduced us to the methods of CV coupled with *in situ* conductance and spectroscopy measurements. Discussions with C Dingler, D Neusser, S Liu and Dr M Goll are highly acknowledged.

ORCID iDs

Sabine Ludwigs https://orcid.org/0000-0002-6717-8538

References

[1] Rivnay J, Inal S, Salleo A, Róisín M O, Berggren M and Malliaras G 2018 Organic electrochemical transistors *Nat. Rev. Mater.* **3** 17086
[2] Swager T M 2017 50th anniversary perspective: conducting/semiconducting conjugated polymers. A personal perspective on the past and the future *Macromol.* **50** 4867–86
[3] Inal S, Rivnay J, Leleux P, Ferro M, Ramuz M, Brendel J C, Schmidt M M, Thelakkat M and Malliaras G G 2014 A high transconductance accumulation mode electrochemical transistor *Adv. Mater.* **26** 7450–5
[4] Elschner A 2011 *PEDOT: Principles and Applications of an Intrinsically Conductive Polymer* (Boca Raton, Florida: CRC Press)
[5] Zotti G and Schiavon G 1989 Spectroclectrochemical determination of polarons in polypyrrole and polyaniline *Synth. Met.* **30** 151–8
[6] Kittlesen G P, White H S and Wrighton M S 1984 Chemical derivatization of microelectrode arrays by oxidation of pyrrole and N-methylpyrrole: fabrication of molecule-based electronic devices *J. Am. Chem. Soc.* **106** 7389–96
[7] Iwasaki Y and Morita M 1995 *Electrochemical Measurements with Interdigitated Array Microelectrodes Current Separations* **14** 2–8
[8] Sezer E, Skompska M and Heınze J 2008 Voltammetric, EQCM, and *in situ* conductance studies of p- and n-dopable polymers based on ethylenedioxythiophene and bithiazole *Electrochim. Acta* **53** 4958–68
[9] Csahok E, Vieil E and Inzelt G 2000 *In situ* dc conductivity study of the redox transformations and relaxation of polyaniline films *J. Electroanal. Chem.* **482** 168–77
[10] Zotti G, Zecchin S, Schiavon G, Berlin A, Pagani G and Canavesi A 1995 Conductivity in redox modified conducting polymers. 2. Enhanced redox conductivity in ferrocene-substituted polypyrroles and polythiophenes *Chem. Mater.* **7** 2309–15
[11] Zotti G, Marin R A and Gallazzi M C 1997 Electrochemical polymerization of mixed Alkyl-Alkoxybithiophenes and -terthiophenes. Substitution-driven polymerization from thiophene hexamers to long-chain polymers *Chem. Mater.* **9** 2945–50
[12] Link S, Richter T, Yurchenko O, Heinze J and Ludwigs S 2010 Electrochemical behavior of electropolymerized and chemically synthesized hyperbranched polythiophenes *J. Phys. Chem.* B **114** 10703
[13] Heinze J, Frontana-Uribe B A and Ludwigs S 2010 Electrochemistry of conducting polymers–persistent models and new concepts *Chem. Rev.* **110** 4724–71
[14] Salinas G and Frontana-Uribe B A 2019 Analysis of conjugated polymers conductivity by *in situ* electrochemical-conductance method *Chem. Electro. Chem.* **6** 4105–17
[15] Yurchenko O, Heinze J and Ludwigs S 2010 Electrochemically induced formation of independent conductivity regimes in polymeric tetraphenylbenzidine systems *Chem. Phys. Chem.* **11** 1637–40
[16] Blanchard P, Malacrida C, Cabanetos C, Roncali J and Ludwigs S 2019 Triphenylamine and some of its derivatives as versatile building blocks for organic electronic applications *Polym. Int.* **68** 589–606
[17] Zotti G, Zecchin S, Schiavon G, Louwet F, Groenendaal L, Crispin X, Osikowicz W, Salaneck W and Fahlman M 2003 Electrochemical and XPS studies toward the role of monomeric and polymeric sulfonate counterions in the synthesis, composition, and properties of poly(3,4-ethylenedioxythiophene) *Macromol.* **36** 3337–44
[18] Hsiao Y-S, Whang W-T, Chen C-P and Chen Y-C 2008 High-conductivity poly(3,4-ethylenedioxythiophene): poly(styrene sulfonate) film for use in ITO-free polymer solar cells *J. Mater. Chem.* **18** 5948–4
[19] Li X-Y, Zhang L-P, Tang F, Bao Z-M, Lin J, Li Y-Q, Chen L and Ma C-Q 2016 The solvent treatment effect of the PEDOT: PSS anode interlayer in inverted planar perovskite solar cells *RSC Adv.* **6** 24501–7
[20] Levermore P A, Jin R, Wang X, Chen L, Bradley D D C and Mello J C de 2008 High efficiency organic light-emitting diodes with PEDOT-based conducting polymer anodes *J. Mater. Chem.* **18** 4414–20
[21] Rivnay J, Inal S, Collins B A, Sessolo M, Stavrinidou E, Strakosas X, Tassone C, Delongchamp D M and Malliaras G G 2016 Structural control of mixed ionic and electronic transport in conducting polymers *Nat. Commun.* **7** 11287
[22] Volkov A V, Wijeratne K, Mitraka E, Ail U, Zhao D, Tybrandt K, Andreasen J W, Berggren M, Crispin X and Zozoulenko I V 2017 Understanding the capacitance of PEDOT: PSS *Adv. Funct. Mater.* **27** 1700329
[23] Modarresi M, Franco-Gonzalez J F and Zozoulenko I 2019 Computational microscopy study of the granular structure and pH dependence of PEDOT:PSS *Phys. Chem. Chem. Phys.* **21** 6699–711
[24] Wong W-Y, Wang X, Zhang H-L, Cheung K-Y, Fung M-K, Djurišić A B and Chan W-K 2008 Synthesis, characterization and photovoltaic properties of a low-bandgap platinum(II) polyyne functionalized with a 3,4-ethylenedioxythiophene-benzothiadiazole hybrid spacer *J. Organomet. Chem.* **693** 3603–12
[25] Chahma M'h, Gilroy J B and Hicks R G 2007 Linear and branched electroactive polymers based on ethylenedioxythiophene–triarylamine conjugates *J. Mater. Chem.* **17** 4768
[26] Villeret B and Nechtschein M 1989 Memory effects in conducting polymers *Phys. Rev. Let.* **63** 1285–7
[27] Pei Q, Zuccarello G, Ahlskog M and Inganäs O 1994 Electrochromic and highly stable poly(3,4-ethylenedioxythiophene) switches between opaque blue-black and transparent sky blue *Polymer* **35** 1347–51
[28] Bruchlos K, Trefz D, Hamidi-Sakr A, Brinkmann M, Heinze J, Ruff A and Ludwigs S 2018 Poly(3-hexylthiophene) revisited—Influence of film deposition on the electrochemical behaviour and energy levels *Electrochim. Acta* **269** 299–311
[29] Gabrielli C, García-Jareño J J, Keddam M, Perrot H and Vicente F 2002 Ac-electrogravimetry study of electroactive thin films. I. Application to prussian blue *J. Phys. Chem.* B **106** 3182–91
[30] Bard A and Stratmann M (ed) 2004 *Encyclopedia of Electrochemistry* 8th edn (Weinheim, Germany: Wiley-VCH)
[31] Harman D G, Gorkin R, Stevens L, Thompson B, Wagner K, Weng B, Chung J H Y, in Het Panhuis M and Wallace G G 2015 Poly(3,4-ethylenedioxythiophene):dextran sulfate (PEDOT: DS)—a highly processable conductive organic biopolymer *Acta Biomater.* **14** 33–42
[32] Ouyang J, Xu Q, Chu C-W, Yang Y, Li G and Shinar J 2004 On the mechanism of conductivity enhancement in poly(3,4-ethylenedioxythiophene): poly(styrene sulfonate) film through solvent treatment *Polymer* **45** 8443–50
[33] Wei Q, Mukaida M, Naitoh Y and Ishida T 2013 Morphological change and mobility enhancement in PEDOT: PSS by adding co-solvents *Adv. Mater.* **25** 2831–6

[34] Shi W, Yao Q, Qu S, Chen H, Zhang T and Chen L 2017 Micron-thick highly conductive PEDOT films synthesized via self-inhibited polymerization: roles of anions *NPG Asia Mater.* **9** e405–405
[35] Gustafsson J C, Liedberg B and Inganäs O 1994 *In situ* spectroscopic investigations of electrochromism and ion transport in a poly(3,4-ethylenedioxythiophene) electrode in a solid state electrochemical cell *Solid State Ionics* **69** 145–52
[36] Zozoulenko I, Singh A, Singh S K, Gueskine V, Crispin X and Berggren M 2018 Polarons, Bipolarons, And Absorption Spectroscopy of PEDOT *ACS Appl. Polym. Mater.* **1** 83–94
[37] Marzocchi M, Gualandi I, Calienni M, Zironi I, Scavetta E, Castellani G and Fraboni B 2015 Physical and electrochemical properties of PEDOT:PSS as a tool for controlling cell growth *ACS Appl. Mater. Interf.* **7** 17993–8003
[38] Alemu D, Wei H-Y, Ho K-C and Chu C-W 2012 Highly conductive PEDOT:PSS electrode by simple film treatment with methanol for ITO-free polymer solar cells *Energy Environ. Sci.* **5** 9662–71
[39] Wang G-F, Tao X-M, Xin J H and Fei B 2009 Modification of conductive polymer for polymeric anodes of flexible organic light-emitting diodes *Nanoscale Res. Lett.* **4** 613–7
[40] Stöcker T, Köhler A and Moos R 2012 Why does the electrical conductivity in PEDOT: PSS decrease with PSS content? A study combining thermoelectric measurements with impedance spectroscopy *J. Polym. Sci. B Polym. Phys.* **50** 976–83
[41] Kim N, Kee S, Lee S H, Lee B H, Kahng Y H, Jo Y-R, Kim B-J and Lee K 2014 Highly conductive PEDOT:PSS nanofibrils induced by solution-processed crystallization *Adv. Mater.* **26** 2268–72
[42] Kim S-M *et al* 2018 Influence of PEDOT:PSS crystallinity and composition on electrochemical transistor performance and long-term stability *Nat. Commun.* **9** 3858
[43] Ju D, Kim D, Yook H, Han J W and Cho K 2019 Controlling electrostatic interaction in PEDOT: PSS to overcome thermoelectric tradeoff relation *Adv. Funct. Mater.* **5** 1905590
[44] Fan B, Mei X and Ouyang J 2008 Significant conductivity enhancement of conductive poly(3,4-ethylenedioxythiophene): poly(styrenesulfonate) films by adding anionic surfactants into polymer solution *Macromol.* **41** 5971–3
[45] Song C and Swager T M 2005 Highly conductive poly (phenylene thienylene)s: M -phenylene linkages are not always bad *Macromol.* **38** 4569–76
[46] Lapkowski M and Pron A 2000 Electrochemical oxidation of pedot—*in situ* conductivity and spectroscopic investigations *Synth. Met.* **110** 79–83
[47] Ofer D, Crooks R M and Wrighton M S 1990 Potential dependence of the conductivity of highly oxidized polythiophenes, polypyrroles, and polyaniline: finite windows of high conductivity *J. Am. Chem. Soc.* **112** 7869–79
[48] Zotti G and Schiavon G 1991 Spin and spinless conductivity in polypyrrole. Evidence for Mixed-valence conduction *Chem. Mater.* **3** 62–5
[49] Bredas J L and Street G B 1985 Polarons, bipolarons, and solitons in conducting polymers *Acc. Chem. Res.* **18** 309–15
[50] Golba S, Starczewska O and Idzik K 2015 Electrochemical and spectrophotometric properties of polymers based on derivatives of di- and triphenylamines as promising materials for electronic applications *Des. Monomers Polym.* **18** 770–9
[51] Trefz D, Ruff A, Tkachov R, Wieland M, Goll M, Kiriy A and Ludwigs S 2015 Electrochemical investigations of the N-type semiconducting polymer P(NDI2OD-T2) and its monomer: new insights in the reduction behavior *J. Phys. Chem.* C **119** 22760–71
[52] Izuhara D and Swager T M 2009 Poly(pyridinium phenylene)s: water-soluble N-type polymers *J. Am. Chem. Soc.* **131** 17724–5
[53] Shomura R, Sugiyasu K, Yasuda T, Sato A and Takeuchi M 2012 Electrochemical generation and spectroscopic characterization of charge carriers within isolated planar polythiophene *Macromol.* **45** 3759–71
[54] Benincori T *et al* 2018 Electrochemical studies of a new, low-band gap inherently chiral ethylenedioxythiophene-based oligothiophene *Electrochim. Acta* **284** 513–25
[55] John H, Bauer R, Espindola P, Sonar P, Heinze J and Müllen K 2005 3D-Hybridnetzwerke aus terthiophenfunktionalisierten Polyphenylendendrimeren mit einstellbarer elektrischer Leitfähigkeit *Angew. Chem.* **117** 2501–5